

2008

# Constraints on First-Light Ionizing Sources from Optical Depth of the Cosmic Microwave Background

J Shull

Aparna Venkatesan

*University of San Francisco*, [avenkatesan@usfca.edu](mailto:avenkatesan@usfca.edu)

Follow this and additional works at: <http://repository.usfca.edu/phys>

 Part of the [Astrophysics and Astronomy Commons](#), and the [Physics Commons](#)

---

## Recommended Citation

Shull, J., & Venkatesan, A. (2008). Constraints on first-light ionizing sources from optical depth of the cosmic microwave background. *Astrophysical Journal*, 685(1), 1-7. doi:10.1086/590898

This Article is brought to you for free and open access by the College of Arts and Sciences at USF Scholarship: a digital repository @ Gleeson Library | Geschke Center. It has been accepted for inclusion in Physics and Astronomy by an authorized administrator of USF Scholarship: a digital repository @ Gleeson Library | Geschke Center. For more information, please contact [repository@usfca.edu](mailto:repository@usfca.edu).

## CONSTRAINTS ON FIRST-LIGHT IONIZING SOURCES FROM OPTICAL DEPTH OF THE COSMIC MICROWAVE BACKGROUND

J. MICHAEL SHULL AND APARNA VENKATESAN<sup>1</sup>

University of Colorado, Department of Astrophysical and Planetary Sciences, CASA, 389-UCB, Boulder, CO 80309;  
michael.shull@colorado.edu, avenkatesan@usfca.edu

Received 2006 August 4; accepted 2008 June 4

### ABSTRACT

We examine the constraints on high-redshift star formation, ultraviolet and X-ray preionization, and the epoch of reionization at redshift  $z_r$ , inferred from the recent *WMAP*-5 measurement,  $\tau_e = 0.084 \pm 0.016$ , of the electron-scattering optical depth of the cosmic microwave background (CMB). Half of this scattering can be accounted for by the optical depth,  $\tau_e = 0.04\text{--}0.05$ , of a fully ionized intergalactic medium (IGM) at  $z \leq z_{\text{GP}} \approx 6\text{--}7$ , consistent with Gunn-Peterson absorption in neutral hydrogen. The required additional optical depth,  $\Delta\tau_e = 0.03 \pm 0.02$  at  $z > z_{\text{GP}}$ , constrains the ionizing contributions of “first light” sources. *WMAP*-5 also measured a significant increase in small-scale power, which lowers the required efficiency of star formation and ionization from minihalos. Early massive stars (UV radiation) and black holes (X-rays) can produce a partially ionized IGM, adding to the residual electrons left from incomplete recombination. Inaccuracies in computing the ionization history,  $x_e(z)$ , and degeneracies in cosmological parameters ( $\Omega_m$ ,  $\Omega_b$ ,  $\sigma_8$ ,  $n_s$ ) add systematic uncertainty to the measurement and modeling of  $\tau_e$ . From the additional optical depth from sources at  $z > z_{\text{GP}}$ , we limit the star formation efficiency, the rate of ionizing photon production for Population III and Population II stars, and the photon escape fraction, using standard histories of baryon collapse, minihalo star formation, and black hole X-ray preionization.

*Subject headings:* cosmic microwave background — cosmology: theory — intergalactic medium

### 1. INTRODUCTION

In recent years, an enormous amount of exciting cosmological data have appeared, accompanied by theoretical inferences about early galaxy formation and the first massive stars. Many of these inferences were reactions to first-year results from the *Wilkinson Microwave Anisotropy Probe* (*WMAP*; Kogut et al. 2003; Spergel et al. 2003). These results (*WMAP*-1) implied a high optical depth to the cosmic microwave background (CMB) and suggested early reionization of the intergalactic medium (IGM). Other conclusions came from simplified models for the stellar initial mass function (IMF), atomic/molecular physics, radiative processes, and prescriptions for star formation rates and escape of photoionizing radiation from protogalaxies.

The CMB optical depth and other cosmological parameters have been refined significantly in the recent five-year *WMAP* data (Hinshaw et al. 2008). In this paper, we use these new measurements to constrain the efficiency of first-light ionizing sources. We focus on the reionization epoch, defined as the redshift  $z_r$  when the IGM becomes nearly fully ionized over most of its volume (Gnedin 2000, 2004). Our knowledge about reionization comes primarily from three types of observations: hydrogen Ly $\alpha$  absorption in the IGM, high- $z$  Ly $\alpha$ -emitting galaxies, and CMB optical depth. Optical spectroscopic studies of the “Gunn-Peterson” (Ly $\alpha$ ) absorption toward high-redshift quasars and galaxies imply that H I reionization occurred not far beyond  $z_{\text{GP}} \sim 6$  (Becker et al. 2001; Fan et al. 2002, 2006). Ultraviolet spectra suggest that He II reionization occurred at  $z \sim 3$  (Kriss et al. 2001; Shull et al. 2004; Zheng et al. 2004). The detection of high-redshift (Ly $\alpha$ -emitting) galaxies (Hu & Cowie 2006) suggests a somewhat higher redshift,  $z_r \geq 6.5$ . Data from *WMAP*, after three years (Spergel et al. 2007) and five years (Hinshaw et al. 2008), suggest

that reionization might occur at  $z \approx 10$ , with sizeable uncertainties in measuring and modeling the CMB optical depth.

There appears to be a discrepancy between the two epochs,  $z_{\text{GP}} \approx 6\text{--}7$  and  $z_r \approx 10$ . However, the *WMAP* and Ly $\alpha$  absorption results are not necessarily inconsistent, since they probe small amounts of ionized and neutral gas, respectively. Both the H I absorbers and ionized filaments in the “cosmic web” (Cen & Ostriker 1999) are highly structured at redshifts  $z < 10$  and affect the optical depths in Ly $\alpha$ . In order to effectively absorb all the Ly $\alpha$  radiation at  $z \approx 6$ , a volume-averaged neutral fraction of just  $x_{\text{H I}} \approx 4 \times 10^{-4}$  is required (Fan et al. 2006). Simulations of the reionization process (Gnedin 2004; Gnedin & Fan 2006) show that the transition from neutral to ionized is extended in time between  $z = 5$  and 10. The first stage (pre-overlap) involves the development and expansion of the first isolated ionizing sources. The second stage marks the overlap of the ionization fronts and the disappearance of the last vestiges of low-density neutral gas. Finally, in the post-overlap stage, the remaining high-density gas is photoionized. The final drop in neutral fraction and increase in photon mean free path occur quite rapidly, over  $\Delta z \approx 0.3$ .

Initial interpretations of the high *WMAP*-1 optical depth ( $\tau_e = 0.17 \pm 0.03$ ) were based on models of “sudden reionization,” neglecting scattering from a partially ionized IGM at  $z > z_r$ . The three-year (*WMAP*-3) and five-year (*WMAP*-5) data resulted in considerable downward revisions, with recent measurements giving  $\tau_e = 0.084 \pm 0.016$  (Hinshaw et al. 2008; Komatsu et al. 2008). These analyses assumed a single step to complete ionization ( $x_e = 1$  at  $z \leq z_r$ ), while Dunkley et al. (2008) also explored a two-step ionization history with a broader distribution of  $\tau_e$ . The *WMAP*-5 data alone gave a  $5\sigma$  detection,  $\tau_e = 0.087 \pm 0.017$  (Dunkley et al. 2008), while *WMAP*-5 combined with distance measurements from Type Ia supernovae (SNe) and baryon acoustic oscillations (BAO) gave  $\tau_e = 0.084 \pm 0.016$  (Hinshaw et al. 2008; Komatsu et al. 2008). The single-step analyses gave a reionization epoch  $z_r = 10.8 \pm 1.4$  at 68% confidence level (C.L.).

<sup>1</sup> Current address: Department of Physics, 2130 Fulton Street, University of San Francisco, San Francisco, CA 94117.

The  $\chi^2$  curves for two-step ionization provide little constraint on the redshift of reionization or on an IGM with low partial ionization fractions,  $x_e \ll 0.1$ , as we discuss in § 3. Figure 3 of Spergel et al. (2007) and Figure 8 of Dunkley et al. (2008) show that the parameters  $x_e$  and  $z_r$  are somewhat degenerate, each with a long tail in the likelihood curves. This emphasizes the importance of contributions to  $\tau_e$  from ionizing UV photons at  $z > z_{\text{GP}}$  from early massive stars and X-rays from accreting black holes (Venkatesan et al. 2001, hereafter VGS01; Ricotti & Ostriker 2004; Begelman et al. 2006).

Models of the extended recombination epoch (Seager et al. 2000) predict a partially ionized medium at high redshifts, owing to residual electrons left from incomplete recombination. Residual electrons produce additional scattering,  $\Delta\tau_e \approx 0.06$ , between redshifts  $z \approx 10$  and 700. These effects are computed in CMB radiation transfer codes such as CMBFAST and RECFAST, but only a portion of this scattering affects the large angular scales ( $l \leq 10$ ) where *WMAP* detects a polarization signal. X-ray preionization can also produce CMB optical depths  $\tau_e \geq 0.01$  (VGS01; Ricotti et al. 2005).

As we discuss in § 2.1, a fully ionized IGM from  $z = 0$  back to  $z_{\text{GP}} = 6.1 \pm 0.15$ , the reionization epoch inferred from Gunn-Peterson absorption (Gnedin & Fan 2006), produces optical depth  $\tau_e \approx 0.041 \pm 0.003$ . This represents nearly half of the *WMAP*-5 measurement,  $\tau_e = 0.084 \pm 0.016$ . If the epoch of Gunn-Peterson reionization is  $z_{\text{GP}} = 7$  (Wyithe et al. 2008), the contribution is  $\tau_e = 0.050 \pm 0.003$ . Therefore, the high-redshift ionizing sources are limited to producing an additional optical depth,  $\Delta\tau_e \leq 0.03 \pm 0.02$ . In § 3, we discuss the resulting constraints on the amount of star formation and X-ray activity at  $z \geq 7$ . We also parameterize the efficiency of various star formation environments, as determined by halo mass and the metallicity of stellar populations, to address several questions. Can reionization occur at relatively low efficiency, corresponding to star formation in massive Ly $\alpha$ -cooled halos (virial temperature  $T_{\text{vir}} \approx 10^4$  K), or must it take place in H<sub>2</sub>-cooled minihalos ( $T_{\text{vir}} \approx 10^3$  K)? Does one require the high ionizing efficiencies of Population III (metal free) stars, or can reionization be achieved by lower efficiency Population II stars?

The IGM is thought to have a complex reionization history, with periods of extended reionization for H I and He II (Venkatesan et al. 2003; Cen 2003; Wyithe & Loeb 2003; Hui & Haiman 2003; Benson et al. 2006). Because  $\tau_e$  measures the integrated column density of electrons, there are many possible scenarios consistent with the *WMAP*-5 data. In addition, reionization models are quite sensitive to the amount of “small-scale power” for ionizing sources, which depend on  $\sigma_8$ , the normalized amplitude of fluctuations.

## 2. OPTICAL DEPTH TO ELECTRON SCATTERING

### 2.1. Analytic Calculation of Optical Depth

To elucidate the dependence of CMB optical depth on the epoch of reionization (redshift  $z_r$ ), we integrate the electron scattering optical depth,  $\tau_e(z_r)$ , for a homogeneous, fully ionized medium out to  $z_r$ . For instantaneous, complete ionization at redshift  $z_r$ , we calculate  $\tau_e$  as the integral of  $n_e\sigma_T dl$ , the electron density times the Thomson cross section along proper length,

$$\tau_e(z_r) = \int_0^{z_r} n_e\sigma_T(1+z)^{-1}[c/H(z)] dz. \quad (1)$$

We adopt a standard  $\Lambda$ CDM cosmology, in which  $(dl/dz) = c(dt/dz) = (1+z)^{-1}[c/H(z)]$ , where  $H(z) = H_0[\Omega_m(1+z)^3 + \Omega_\Lambda]^{1/2}$

and  $\Omega_m + \Omega_\Lambda = 1$  (no curvature). The densities of hydrogen, helium, and electrons are written  $n_{\text{H}} = [(1-Y)\Omega_b\rho_{\text{cr}}/m_{\text{H}}](1+z)^3$ ,  $n_{\text{He}} = yn_{\text{H}}$ , and  $n_e = n_{\text{H}}(1+y)$ , if helium is singly ionized. We assume a primordial helium mass fraction,  $Y = 0.2477 \pm 0.0029$  (Peimbert et al. 2007), and define  $y = (Y/4)/(1-Y) \approx 0.0823$  as the He fraction by number. Helium contributes 8% to  $\tau_e$ , assuming single ionization (He II) at  $z > 3$ . An additional  $\tau_e \approx 0.002$  comes from helium reionization to He III at  $z \leq 3$  (Shull et al. 2004). The critical density is  $\rho_{\text{cr}} = (1.8785 \times 10^{-29} \text{ g cm}^{-3}) h^2$ , where  $h = (H_0/100 \text{ km s}^{-1} \text{ Mpc}^{-1})$ . The above integral can be done analytically:

$$\begin{aligned} \tau_e(z_r) &= \left(\frac{c}{H_0}\right) \left(\frac{2\Omega_b}{3\Omega_m}\right) \left[\frac{\rho_{\text{cr}}(1-Y)(1+y)\sigma_T}{m_{\text{H}}}\right] \\ &\quad \times \left\{ \left[ \Omega_m(1+z_r)^3 + \Omega_\Lambda \right]^{1/2} - 1 \right\} \\ &= (0.00435 h_{70}) \\ &\quad \times \left\{ \left[ (0.2794 h_{70}^{-2})(1+z_r)^3 + 0.7206 \right]^{1/2} - 1 \right\}, \quad (2) \end{aligned}$$

where we write  $(1-Y)(1+y) = (1-3Y/4)$  and use the updated *WMAP*-5 parameters,  $\Omega_b h^2 = 0.02265 \pm 0.00059$  and  $\Omega_m h^2 = 0.1369 \pm 0.0037$ . To this formula we add the extra scattering ( $\tau_e \approx 0.0020$ ) from He III at  $z \leq 3$ . With this He III contribution, equation (2) yields  $\tau_e = 0.040, 0.045$ , and  $0.050$  for  $z_r = 6.0, 6.5$ , and  $7.0$ , respectively.

For large redshifts,  $\Omega_m(1+z)^3 \gg \Omega_\Lambda$ , and the integral simplifies to

$$\begin{aligned} \tau_e(z_r) &\approx \left(\frac{c}{H_0}\right) \left(\frac{2\Omega_b}{3\Omega_m^{1/2}}\right) \left[\frac{\rho_{\text{cr}}(1-3Y/4)\sigma_T}{m_{\text{H}}}\right] (1+z_r)^{3/2} \\ &\approx (0.0522) \left[\frac{(1+z_r)^3}{8}\right]^{1/2}. \quad (3) \end{aligned}$$

Here we have scaled to a reionization epoch  $z_r \approx 7$ . From the approximate expression in equation (3), we see that  $\tau_e \propto (\rho_{\text{cr}}\Omega_b\Omega_m^{-1/2}H_0^{-1})$ . Thus,  $\tau_e$  is nearly independent of the Hubble constant, since  $\rho_{\text{cr}} \propto h^2$  while the combined parameters,  $\Omega_b h^2$  and  $\Omega_m h^2$ , are inferred from D/H, CMB, and large-scale galaxy motions. The scaling with  $h$  therefore cancels to lowest order. A slight dependence remains from the small  $\Omega_\Lambda$  term in equation (2).

If we invert the approximate equation (3), we can estimate the redshift of primary (Gunn-Peterson) reionization,  $(1+z_{\text{GP}}) \approx (7.77)[\tau_e(z_{\text{GP}})/0.05]^{2/3}$ , scaled to the value,  $\tau_e = 0.05$ , expected for full ionization back to  $z_{\text{GP}} \approx 7$ . As discussed in § 2.2, this is approximately the *WMAP*-5 value of optical depth,  $\tau_e = 0.084 \pm 0.016$ , reduced by  $\Delta\tau_e \approx 0.03$ . This additional scattering,  $\Delta\tau_e$ , may arise from high- $z$  star formation, X-ray preionization, and residual electrons left after incomplete recombination. The latter electrons are computed to have fractional ionization  $x_e \approx (0.5-3.0) \times 10^{-3}$  between  $z = 10$  and 700 (Seager et al. 2000). Inaccuracies in computing their contribution therefore add systematic uncertainty to the CMB-derived value of  $\tau_e$ . Partial ionization may also arise from the first stars (Venkatesan et al. 2003, hereafter VTS03) and from penetrating X-rays produced by early black holes (VGS01; Ricotti & Ostriker 2004, 2005). For complete sudden reionization, Komatsu et al. (2008) estimated  $z_r \approx 10.8 \pm 1.4$  at 68% C.L., by combining *WMAP*-5 data with other distance measures (SNe, BAO). The *WMAP*-5 data alone (Dunkley et al. 2008) imply  $\tau_e = 0.087 \pm 0.017$ , with  $z_r = 11.0 \pm 1.4$

(68% C.L.). Their likelihood curves allow a range  $7.5 \leq z_r \leq 13.0$  at 95% C.L. They also claim that *WMAP*-5 data exclude  $z_r = 6$  at more than 99.9% C.L.

The additional ionization sources at  $z > z_{\text{GP}}$  will contribute electron scattering that may bring the *WMAP* and Gunn-Peterson results into agreement for the epoch of complete reionization. In our calculations, described in § 3, we make several key assumptions. First, we assume a fully ionized IGM out to  $z_{\text{GP}} \approx 6\text{--}7$ , accounting for both  $\text{H}^+$  and ionized helium. Second, we investigate the effects of IGM partial ionization at  $z > z_{\text{GP}}$ . Finally, in computing the contribution of residual electrons at high redshifts, we adopt the concordance parameters from the *WMAP*-5 data set. The CMB optical depth is formally a  $5\sigma$  result, which may improve as *WMAP* refines its estimates of the matter density,  $\Omega_m$ , and the parameters,  $\sigma_8$  and  $n_s$ , that govern small-scale power. Both  $\sigma_8$  and  $n_s$  have well-known degeneracies with  $\tau_e$  in CMB parameter extraction (Spergel et al. 2007; Dunkley et al. 2008). The derived parameters may change in future CMB data analyses, as the constraints on  $\tau_e$  continue to evolve. In addition, inaccuracies in the incomplete recombination epoch and residual ionization history,  $x_e(z)$ , add uncertainties to the CMB radiative transfer, the damping of  $l$ -modes, and the polarization signal used to derive an overall  $\tau_e$ .

## 2.2. Residual Electrons in the IGM

We now discuss the contribution of residual electrons in the IGM following the recombination epoch at  $z \approx 1000$ . Scattering from these electrons is significant and is normally accounted for in CMB transport codes such as CMBFAST (Seljak & Zaldarriaga 1996) through the postrecombination IGM ionization history,  $x_e(z)$ . However, a number of past papers are vague on how the ionization history is treated and on precisely which electrons contribute to total optical depth  $\tau_e$ . This has led to confusion in how much residual optical depth and damping of CMB power has been subtracted from the CMB signal. It is important to be clear on the definition of the integrated  $\tau_e$  when using it to constrain the amount of high- $z$  ionization from first-light sources. Modern calculations of how the IGM became neutral have been done by Seager et al. (2000), although their code (RECFAST) continues to be modified to deal with subtle effects of the recombination epoch and the atomic physics of hydrogen ( $ns \rightarrow 1s$  and  $nd \rightarrow 1s$ ) two-photon transitions (Chluba & Sunyaev 2008).

To illustrate the potential effects of high- $z$  residual electrons, we have used numbers from Figure 2 of Seager et al. (2000), the top-panel model, which assumed a cosmology with  $\Omega_{\text{tot}} = 1$ ,  $\Omega_b = 0.05$ ,  $h = 0.5$ ,  $Y = 0.24$ , and  $T_{\text{CMB}} = 2.728$  K. At low redshifts,  $z \approx z_r$ , just before reionization, they find a residual electron fraction  $x_{e,0} \approx 10^{-3.3}$ . We fitted their curve for  $\log x_e$  out to  $z \approx 500$  to the formula

$$x_e(z) = x_{e,0} 10^{0.001(1+z)} \approx (5 \times 10^{-4}) \exp[\alpha(1+z)], \quad (4)$$

where  $\alpha \approx 2.303 \times 10^{-3}$ . More recent recombination calculations (W. Y. Wong & D. Scott 2007, private communication) using *WMAP* parameters ( $\Omega_b = 0.04$ ,  $h = 0.73$ ,  $\Omega_m = 0.24$ ,  $\Omega_\Lambda = 0.76$ ) and  $Y = 0.244$  find somewhat lower values,  $x_{e,0} \approx 10^{-3.67}$  with  $\alpha \approx 2.12 \times 10^{-3}$ . The lower  $x_{e,0}$  and the faster recombination rates arise from their higher assumed baryon density,  $\Omega_b h^2 = 0.0213$ , compared to  $\Omega_b h^2 = 0.0125$  in Seager et al. (2000).

To compute the electron scattering of the CMB from these “frozen out” electrons, we use the same integrated optical depth formula (eq. [1]), in the high- $z$  limit, where  $(dl/dz) = (1+z)^{-1} \times [c/H(z)] \approx (c/H_0)\Omega_m^{-1/2}(1+z)^{-5/2}$ . We integrate over the residual-

TABLE 1  
IONIZATION FRACTIONS AND RESIDUAL OPTICAL DEPTH

Redshift Range	$x_{e,0}^a$	$\alpha^a$	$\Delta\tau_e^b$
$7 < z < 500$ .....	$5.00 \times 10^{-4}$	$2.303 \times 10^{-3}$	0.0256
$500 < z < 600$ .....	$2.94 \times 10^{-4}$	$3.224 \times 10^{-3}$	0.0135
$600 < z < 700$ .....	$1.28 \times 10^{-4}$	$4.606 \times 10^{-3}$	0.021

<sup>a</sup> Parameters for  $x_e(z) = x_{e,0} \exp[-\alpha(1+z)]$  (see text).

<sup>b</sup> Residual integrated optical depth computed over given redshift range (see eq. [5]).

electron history, from  $z_r \approx 7$  back to a final redshift  $z_f \gg z_r$ , to find

$$\begin{aligned} (\Delta\tau_e)_{\text{res}} &= \left(\frac{c}{H_0}\right) \left[ \frac{\rho_{\text{cr}}(1-Y)\sigma_T\Omega_b}{\Omega_m^{1/2}m_{\text{H}}} \right] \int_{z_r}^{z_f} (1+z)^{1/2} x_e(z) dz \\ &= (3.18 \times 10^{-3}) x_{e,0} \int_{(1+z_r)}^{(1+z_f)} u^{1/2} \exp(\alpha u) du. \end{aligned} \quad (5)$$

A rough estimate to the residual scattering comes from setting  $\alpha = 0$  and adopting a constant ionized fraction  $x_e(z)$ ,

$$(\Delta\tau_e)_{\text{res}} \approx (2.12 \times 10^{-3}) \langle x_e \rangle \left[ (1+z_f)^{3/2} - (1+z_r)^{3/2} \right]. \quad (6)$$

This estimate gives  $\tau_e = 0.039$  for  $z_r = 6$ ,  $z_f = 700$ , and  $\langle x_e \rangle \approx 10^{-3}$ . More precise values of  $\tau_e$  can be derived from the exact integral (eq. [5]) by expanding the exponential as a sum and adopting the limit  $z_f \gg z_r$ ,

$$(\Delta\tau_e)_{\text{res}} = (0.0179) \left[ \frac{(1+z_f)}{501} \right]^{3/2} \sum_{n=0}^{\infty} \frac{[\alpha(1+z_f)]^n}{(n+3/2)n!}. \quad (7)$$

For  $z > 500$ , the approximate formula (eq. [4]) underestimates  $x_e$ , but one can integrate the appropriate curves (Seager et al. 2000) using piecewise-continuous linear fits. Table 1 lists the fitting parameters,  $x_{e,0}$  and  $\alpha$ , for various redshift ranges, together with the extra contribution,  $\Delta\tau_e$ . These calculations give a total optical depth in residual electrons  $\Delta\tau_e \approx 0.06$  back to  $z = 700$ . These electrons have maximum influence on angular scales with harmonic  $l_{\text{max}} \approx 2z^{1/2} \approx 20\text{--}50$  (Zaldarriaga 1997). At higher redshifts,  $x_e$  rises to  $10^{-2.1}$  at  $z = 800$  and to  $10^{-1.1}$  at  $z = 1000$ , where the CMB source function will affect the “free streaming” assumption used in CMBFAST (Seljak & Zaldarriaga 1996).

## 3. IMPLICATIONS FOR REIONIZATION MODELS

The *WMAP*-5 measurements (Hinshaw et al. 2008; Komatsu et al. 2008) of fluctuations in temperature ( $T$ ) and polarization ( $E$ ) have been interpreted to estimate total electron-scattering optical depth of  $\tau_e \approx 0.084 \pm 0.016$ . The central value comes from computing the likelihood function for the six-parameter fit to *WMAP*-5 data (correlations  $TT$ ,  $TE$ , and  $EE$ ) marginalized with BAO and SNe distance measures. Because of the challenges in translating a single parameter ( $\tau_e$ ) into a reionization history,  $x_e(z)$ , it is important to recognize the sizable error bars on  $\tau_e$ . At 68% C.L. (Fig. 1 of Komatsu et al. 2008; Fig. 6 of Dunkley et al. 2008), when marginalized against other parameters such as “tilt” ( $n_s$ ), the optical depth ranges from  $\tau_e = 0.06$  to 0.11. The lower value is only slightly above the optical depth,  $\tau_e = 0.05$ , for a

fully ionized IGM back to redshift  $z_{\text{GP}} \approx 7$ . The higher value,  $\tau_e = 0.11$ , clearly requires additional ionizing sources at  $z > z_{\text{GP}}$ .

In § 2.1, we showed that  $\sim 50\%$  of this  $\tau_e$  can be accounted for by a fully ionized IGM at  $z \leq z_{\text{GP}}$ . Observations of Ly $\alpha$  (Gunn-Peterson) absorption toward 19 quasars between  $5.7 < z < 6.4$  (Fan et al. 2006) are consistent with a reionization epoch  $z_r \approx z_{\text{GP}} = 6.1 \pm 0.15$  (Gnedin & Fan 2006). According to equation (2), this produces  $\tau_e = 0.041 \pm 0.003$ , where our error propagation includes relative uncertainties in  $z_r$  (2.5%),  $\Omega_m h^2$  (8.4%), and  $\Omega_b h^2$  (4.0%). Detections of Ly $\alpha$ -emitting galaxies at  $z \approx 6.6$  (Hu et al. 2002; Kodaira et al. 2003; Hu & Cowie 2006) suggest that the epoch of full reionization might be as high as  $z_r \approx 7$ . This reionization epoch corresponds to  $\tau_e \approx 0.05$  and is consistent with the small neutral fraction to which the Gunn-Peterson test is sensitive, particularly when one accounts for density bias in the observed high- $z$  ionization zones around quasars (Wyithe et al. 2008). Residual postrecombination electrons produce a substantial optical depth from  $z \approx 10$  back to  $z \approx 700$ , which uniformly damps all angular scales. However, their effect on the *TE* and *EE* power is considerably less on large angular scales ( $l \leq 10$ ). Thus, we can identify a significant portion of the *WMAP-5* observed optical depth through known sources of ionization. The “visible ionized universe” out to  $z_{\text{GP}} = 6-7$  accounts for  $\tau_e = 0.04-0.05$ , while high- $z$  partial ionization could contribute additional  $\Delta\tau_e \approx 0.01-0.03$ . For this study, we investigate the requirements to produce an additional optical depth,  $\Delta\tau_e = 0.03 \pm 0.02$ , from star formation and early black hole accretion at  $z > z_{\text{GP}}$ .

Our calculations represent an important change in the derivation of  $z_r$  from  $\tau_e$  and suggest that the amount and efficiency of high- $z$  star formation need to be suppressed. This suggestion is ironic, since *WMAP-1* data initially found a high  $\tau_e = 0.17 \pm 0.04$  (Spergel et al. 2003) implying a surprisingly large redshift for early reionization, ranging from  $11 < z_r < 30$  at 95% C.L. (Kogut et al. 2003). These results precipitated many investigations of star formation at  $z = 10-30$ , some of which invoked anomalous mass functions, very massive stars (VMSs, with  $M > 140 M_\odot$ ), and an increased ionizing efficiency from zero-metallicity stars (VTS03; Wyithe & Loeb 2003; Cen 2003; Ciardi et al. 2003; Sokasian et al. 2003, 2004). Tumlinson et al. (2004, hereafter TVS04) disputed the hypothesis that the first stars had to be VMSs. They showed that an IMF dominated by  $10-100 M_\odot$  stars can produce the same ionizing photon budget as VMSs, generate CMB optical depths of 0.09–0.14, and still be consistent with nucleosynthetic evidence from extremely metal-poor halo stars (Umeda & Nomoto 2003; Tumlinson 2006; Venkatesan 2006).

Although the IGM recombination history,  $x_e(z)$ , is included in calculations of CMBFAST and in CMB parameter estimation, the best-fit values of  $\tau_e$  from *WMAP-5* and earlier CMB experiments have been attributed exclusively to the contribution from the first stars and/or black holes at  $z \leq 20$ . The contributions from postrecombination electrons ( $20 < z < 1100$ ) have not always been subtracted from the data. This postrecombination contribution was relatively small in some earlier models of reionization (Zaldarriaga 1997; Tegmark & Silk 1995) that explored optical depths of  $\tau_e = 0.5-1.0$  and suggested reionization epochs up to  $z_r \sim 100$ . However, with current data indicating late reionization, it becomes particularly important to consider contributions to  $\tau_e$  at  $z > z_{\text{GP}}$ , prior to the first identified sources of light. The latest *WMAP-5* results (Hinshaw et al. 2008) find a lower  $\tau_e$ , but they also suggest more small-scale power available for reionizing sources, owing to higher normalization parameters,  $\sigma_8 \approx 0.817 \pm 0.026$  and  $\Omega_m h^2 \approx 0.1369 \pm 0.0037$ . This change marks a sig-

nificant increase ( $\Delta\sigma_8 = +0.056$ ) over *WMAP-3* data. Between *WMAP-1* and *WMAP-3*, the decrease in  $\sigma_8$  was offset by a reduction in spectrum tilt. However, this index did not change significantly in the recent data, going from  $n_s = 0.958 \pm 0.016$  (*WMAP-3*) to  $n_s = 0.960^{+0.014}_{-0.013}$  (*WMAP-5*). Alvarez et al. (2006) argued, from the lower values of  $\tau_e$  and  $\sigma_8$ , that both *WMAP-3* and *WMAP-1* data require similar (high) stellar ionizing efficiencies. Haiman & Bryan (2006) use the lower  $\tau_e$  to suggest that massive star formation was suppressed in minihalos. Our results on a lower  $\Delta\tau_e$  make these requirements even more stringent, as we now quantify.

In the next two subsections, we consider two scenarios for producing partial IGM ionization at  $z > z_{\text{GP}}$ . The first considers ionizing UV photons from the first massive stars, which will create small “bubbles” of fully ionized gas inside ionization fronts. The second scenario examines extended partial ionization produced by X-rays from accreting black holes.

### 3.1. Ionization by Hot Stars

Semianalytic and numerical models of reionization (Ricotti et al. 2002a, 2002b; VTS03, Haiman & Holder 2003) show that the efficiency of ionizing photon injection into the IGM can be parameterized by the production rate of ionizing (UV) photons from massive stars. In our approximate models, we compute the hydrogen ionization fraction as  $x_e(z) = \epsilon_{\text{UV}} f_b(z) / c_L(z)$ , where  $\epsilon_{\text{UV}} = N_\gamma f_* f_{\text{esc}}$  and  $f_b(z)$  is the fraction of baryons in collapsed halos. The free parameters in this model are encapsulated in the “triple product,”  $f_* N_\gamma f_{\text{esc}}$ , where  $f_*$  represents the star formation efficiency (the fraction of a halo’s baryons that go into stars),  $N_\gamma$  is the number of ionizing photons produced per baryon of star formation, and  $f_{\text{esc}}$  is the fraction of these ionizing photons that escape from the halo into the IGM.

To account for the nonlinearity of recombinations, we define  $c_L \equiv \langle n_{\text{H II}}^2 \rangle / \langle n_{\text{H II}} \rangle^2$ , the space-averaged clumping factor of ionized hydrogen. We assume that  $c_L$  is the same for H II and He III and that  $N_\gamma f_* f_{\text{esc}}$  is constant with redshift. As discussed by Gnedin & Ostriker (1997), particularly in their § 3.1, clumping of the photoionized gas sharpens the reionization transition, with a recombination time much less than the local Hubble time at  $z \approx 6-8$ . However, the integrated optical depth through this epoch is not greatly affected by clumping.

The main effects of clumping arise when we translate the production rate of ionizing photons into the ionization history,  $x_e(z)$ . When the local density of photoionized hydrogen is close to ionization equilibrium,  $\langle n_{\text{H II}} \Gamma_{\text{H I}} \rangle \approx \langle \alpha_{\text{H}}^{(A)}(T) n_e n_{\text{H II}} \rangle$ , and the quadratic dependence of recombination rates reduces the local ionization fraction by a factor  $c_L^{-1}$ . When the medium is out of equilibrium, either ionizing or recombining, this approximation,  $x_e(z) = \epsilon_{\text{UV}} f_b(z) / c_L(z)$ , is less accurate. To assess the validity of our approximation, we have run a set of reionization models, integrating differential equations for the propagation of ionization fronts (VTS03) to derive  $x_e(z)$ . When we apply our approximation with  $c_L = 10$ , it closely approximates the integrated hydrogen ionization history with a clumping factor of  $c_L = 40$ . These two curves are virtually indistinguishable for nearly all the redshifts approaching reionization. Thus, an artificial boost by a factor of 4 in the clumping factor would correct for any deviations in our approximation from the true ionization history. Our approximation is not dramatically different in shape from the true ionization history, at least from our semianalytic calculation, and requires at most a constant multiplicative correction in the clumping factor. We are currently pursuing numerical experiments to understand the relationship between clumping and reionization, using adaptive mesh refinement simulations (Hallman et al. 2007)

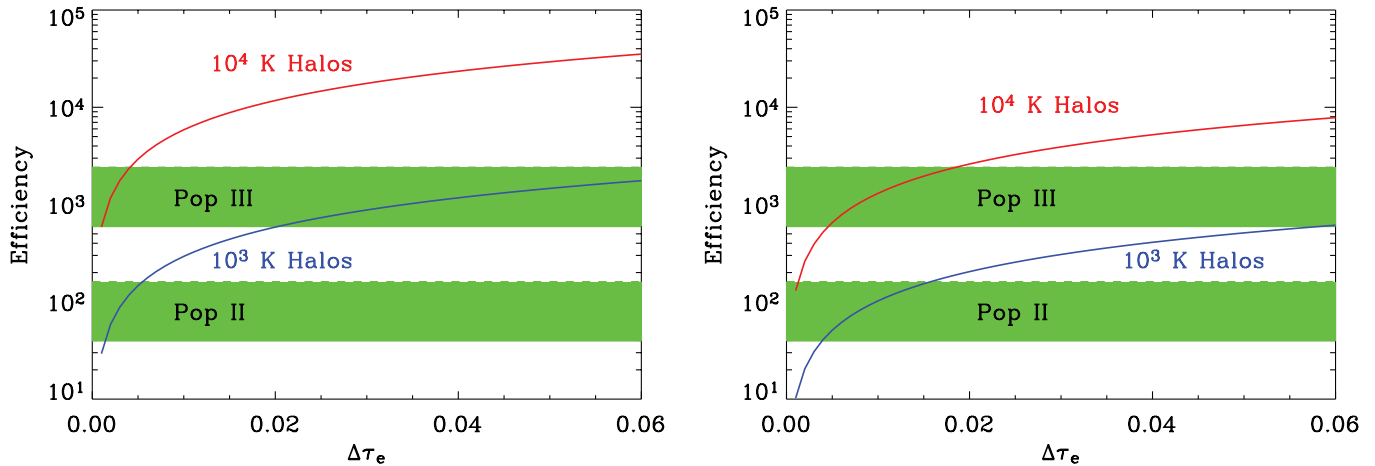


FIG. 1.—Locus of efficiency factors,  $\epsilon_{\text{UV}} = N_\gamma f_* f_{\text{esc}}$ , for production and escape of photoionizing radiation vs. additional optical depth,  $\Delta\tau_e$ , from hot stars at  $z > z_{\text{GP}}$ . Models assume cosmological parameters from *WMAP-3* (left) and *WMAP-5* (right). *WMAP-5* found more small-scale power (higher  $\sigma_8$ ) for minihalo ionization, hence lower required efficiencies. Efficiency,  $\epsilon_{\text{UV}} = f_* N_\gamma f_{\text{esc}}$ , is defined (§ 3.1) for star formation in Ly $\alpha$ -cooled massive halos (red curve,  $T_{\text{vir}} \geq 10^4$  K) and in H $_2$ -cooled minihalos (blue curve,  $T_{\text{vir}} \geq 10^3$  K). Green horizontal bands correspond to expected efficiencies for a Salpeter stellar IMF:  $\epsilon_{\text{UV}} \approx 600\text{--}2000$  for metal-free Pop III (10–140  $M_\odot$ ) and  $\epsilon_{\text{UV}} \approx 40\text{--}150$  for metal-enriched Pop II (1–100  $M_\odot$ ). We adopt star formation efficiency  $f_* = 0.1$  and photon escape fraction  $f_{\text{esc}}$  ranging from 0.1 to 0.4 (see § 3.1 for details). The intersection of the rising red curve in the right panel with the upper green band shows that Pop III halos ( $T_{\text{vir}} \approx 10^4$  K) can produce  $\Delta\tau_e \approx 0.01\text{--}0.02$ . The intersection of the rising blue curve with the two bands shows that minihalos ( $T_{\text{vir}} \approx 10^3$  K) can produce  $\Delta\tau_e = 0.01\text{--}0.02$  (Pop II) and  $\Delta\tau_e$  up to 0.06 (Pop III/Pop II).

and exploring different weighting schemes for clumping on the subgrids.

We can now use our calculations to constrain the amount of high- $z$  star formation through the product of these three parameters. We solve for the ionization history, using our previous formalism (VTS03) in which the baryon collapse history,  $f_b(z)$ , is computed through the Press-Schechter formalism with the cosmological parameters from *WMAP-5*. The propagation of ionization fronts is followed through the production rate of ionizing photons minus recombinations.

Each of these three parameters has some dependence on the halo mass and environment (Haiman & Bryan 2006; Ricotti & Shull 2000). Since we have already parameterized the intrahalo recombinations through  $f_{\text{esc}}$ , we account for the loss of ionizing photons on IGM scales through  $c_L$  in two forms: (1) a power-law form with slope  $\beta = -2$  from the semianalytic work of Haiman & Bryan (2006); and (2) the numerical simulations of Kohler et al. (2007), using their case C (overdensity  $\delta \sim 1$  for the large-scale IGM) for  $C_R$ , the recombination clumping factor corresponding to our definition of  $c_L$ . In the latter case, the clumping factor is almost constant ( $c_L \approx 6$ ) until the very end of reionization. Together, these two different cases provide bounds on the range of possible values, although they are quite similar over the epoch  $z \approx 6\text{--}8$  that dominates the scattering. In our calculations, we use the Haiman & Bryan (2006) formulation of  $C_L(z)$ .

With these assumptions, we can use equation (5) and the allowed additional optical depth,  $\Delta\tau_e \leq 0.03$ , to constrain the ionizing efficiency of the first stars. In Figure 1, we plot curves of efficiency factor,  $\epsilon_{\text{UV}}$ , as a function of the resulting  $\Delta\tau_e$ . The two panels illustrate the changes in required efficiency produced by the *WMAP-5* increase in “small-scale power” compared to *WMAP-3* parameters. These differences arise primarily from the amplitude of fluctuations,  $\sigma_8$ , which increased from  $\sigma_8 = 0.761^{+0.049}_{-0.048}$  (*WMAP-3*) to  $\sigma_8 = 0.817 \pm 0.026$  (*WMAP-5*). In each panel, we show two curves, corresponding to star formation in Ly $\alpha$ -cooled halos, with virial temperature  $T_{\text{vir}} \approx 10^4$  K, and in H $_2$ -cooled minihalos ( $T_{\text{vir}} \approx 10^3$  K). For these calculations, we adopt the clumping factors from Haiman & Bryan (2006), a star formation efficiency  $f_* = 0.1$ , and a range of escape fractions  $f_{\text{esc}} = 0.1\text{--}0.4$ . The two curves (red and blue) illustrate cases designated

as Population II (Pop II, metal enriched) and Population III (Pop III, zero metal) stars. Both models adopt Salpeter initial mass functions (IMF), for which we find (1)  $N_\gamma = 60,000$  for a metal-free IMF (10–140  $M_\odot$ ) that agrees with both CMB and nucleosynthetic data (TVS04), and (2)  $N_\gamma = 4000$  for a present-day IMF (1–100  $M_\odot$ ). Note that  $N_\gamma = 34,000$  is consistent with  $\tau_e \approx 0.084 \pm 0.016$  (*WMAP-5*) if photons arise from zero-metal stars (Tumlinson 2006). Values of  $N_\gamma$  were derived (TVS04) from the lifetime-integrated ionizing photon production from various stellar populations and IMFs and used as inputs in reionization models.

Figure 1 shows how the required additional optical depth,  $\Delta\tau_e = 0.03 \pm 0.02$ , translates into the efficiency required of massive stars forming in high- $z$  halos. These plots are meant to be used as indicators of the types of star-forming halos and the stellar populations that generate ionizing photons, per baryon that passes through stars. The two panels also illustrate the sensitivity of the efficiencies to cosmological parameters (*WMAP-3* vs. *WMAP-5*), primarily the amplitude of fluctuations,  $\sigma_8$ , which sets the small-scale power of halos at a given epoch. The interpretation of Figure 1 comes from the intersection of the two rising curves (red curve, massive halos; blue curve, minihalos) with the two green bands, which mark the range of expected efficiencies of Pop II and Pop III stars.

One can draw several general conclusions from Figure 1. First, the higher amplitude of small-scale power (larger  $\sigma_8$ ) in the *WMAP-5* results (right) shifts both red and blue curves to the right. Lower efficiencies of ionizing photon production are required to produce a given additional optical depth,  $\Delta\tau_e$ . Second, considering just the *WMAP-5* parameters (right), we see that “massive halos,” defined as those with  $T_{\text{vir}} \approx 10^4$  K, can produce optical depths ranging from  $\Delta\tau_e = 0.005$  to 0.018, for a range of Pop III efficiencies  $\epsilon_{\text{UV}} = 600\text{--}2000$ . If one invokes more plentiful minihalos ( $T_{\text{vir}} \approx 10^3$  K), reionization by Pop II stars can produce a similar  $\Delta\tau_e = 0.004\text{--}0.016$ . These results suggest that partial reionization at  $z > z_{\text{GP}}$  could be achieved by minihalos ( $T_{\text{vir}} \approx 10^3$  K), with a mixture of Pop III and Pop II stars, or a transition from one to the other, for which the rising blue curve gives  $\Delta\tau_e \approx 0.02\text{--}0.06$  for  $f_{\text{esc}} = 0.1\text{--}0.4$ . For these minihalos, Pop II stars produce  $\tau \leq 0.02$ , but  $\tau \approx 0.02\text{--}0.06$  can

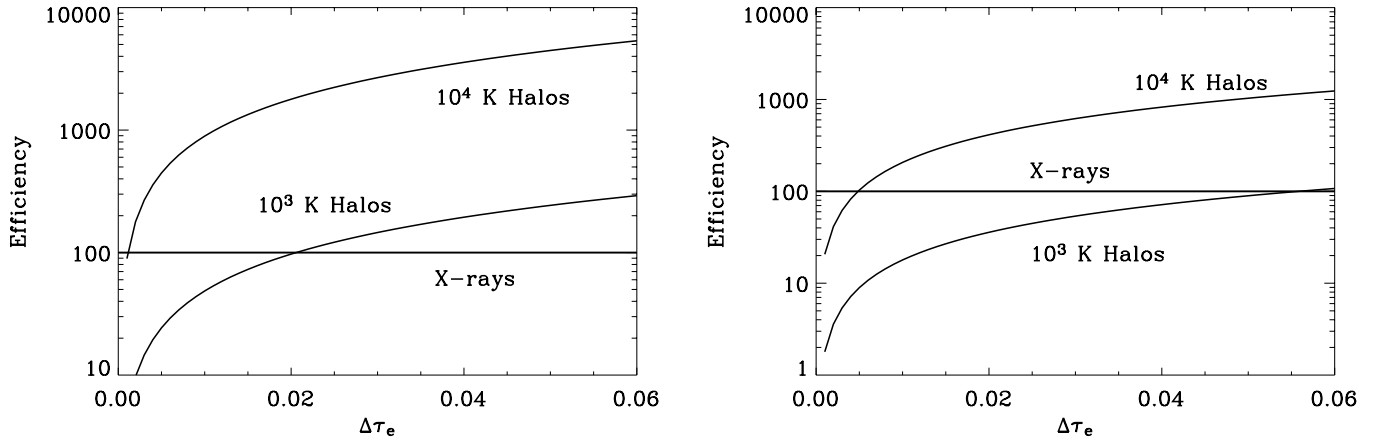


FIG. 2.—X-ray production efficiency,  $\epsilon_X = N_X f_{\text{BH}} f_{\text{esc}}$ , required to produce additional optical depth,  $\Delta\tau_e$ , at  $z > z_{\text{GP}}$ . We assume that  $f_{\text{esc}} = 1$  for X-rays. This efficiency is the product of the baryon fraction in black holes times the total ionizations produced per accreted baryon. Curves are for *WMAP-3* (left) and *WMAP-5* (right) parameters. The required efficiencies are lower for *WMAP-5* parameters, with their additional small-scale power. Two curves are shown, for halos with virial temperatures of  $10^3$  and  $10^4$  K. Horizontal curves show a fiducial value,  $\epsilon_X \approx 100$ , equivalent to  $f_{\text{BH}} \approx 10^{-4}$ ,  $N_X \approx 10^6$  (see § 3.2), and  $f_{\text{esc}} = 1$ .

be achieved either by metal-poor stellar populations in halos with unusually high  $f_*$  or  $f_{\text{esc}}$ , or by metal-free massive stars in halos with very low star formation rates and/or escape fraction of ionizing radiation.

Another robust conclusion from Figure 1 is that minihalos ( $T_{\text{vir}} = 10^3$  K) with Pop III stars can easily account for the *entire* additional optical depth ( $\Delta\tau_e \approx 0.03$ ) needed to explain the *WMAP-5* data. Even in cases where reionization begins with Pop III stars (efficiencies  $\sim 10^3$ ) and then transitions to Pop II (efficiencies  $\sim 10^2$ ), the optical depths are significant. This is an important astrophysical issue, since the duration of the epoch dominated by metal-free massive first stars is still uncertain (TVS04). These results mark a significant departure from similar curves for a *WMAP-3* cosmology (left), owing to the increased small-scale power in a *WMAP-5* cosmology relative to *WMAP-3*. Although the scalar spectral index  $n_s$  did not change appreciably from year three to year five of *WMAP*, both the matter density,  $\Omega_m$ , and the normalization,  $\sigma_8$ , rose by several percent, an appreciable effect for power available for low-mass halos. Thus, reionization occurs slightly earlier in a *WMAP-5* cosmology ( $\Delta z_r \approx 1-2$ ) in our models, lowering the required efficiencies by a factor of about 4.

Our predictions can be compared to those of Haiman & Bryan (2006), who used *WMAP-3* data to constrain the efficiency factor,  $\epsilon_{\text{UV}}$ , relative to a fiducial value  $\epsilon_{\text{mini}} = 200$  for minihalos. They argued that the efficiency for the production of ionizing photons must have been reduced by an order of magnitude, in order to avoid overproducing the optical depth. However, their constraints were based on the *WMAP-3* value,  $\tau_e \approx 0.09$ , whereas half that scattering is accounted for from the fully ionized IGM at  $z < z_{\text{GP}}$ . In our formalism (Fig. 1, right), the efficiency constraints are less severe, and Pop III minihalos can easily produce  $\Delta\tau_e \approx 0.06$  with the expected efficiencies,  $\epsilon_{\text{UV}} \approx 10^3$ . Much larger efficiencies, close to those of metal-free stellar populations, and large values of  $f_*$  and  $f_{\text{esc}}$  are required for larger halos to produce  $\Delta\tau_e \approx 0.02$ . It makes some difference what form is assumed for the clumping factor,  $c_L$ , in constraining the ionizing efficiency of the first stars. The level of shifts in the (red and blue) efficiency curves is comparable to the shifts between *WMAP-3* and *WMAP-5*.

### 3.2. Ionization by Accreting Black Holes

The CMB optical depth also constrains the level of X-ray preionization from high-redshift black holes. Ricotti et al. (2005) were able to produce large optical depths, up to  $\tau_e \approx 0.17$ , using

accreting high- $z$  black holes with substantial soft X-ray fluxes. Their three simulations (labeled M-PIS, M-SN1, and M-SN2) produced hydrogen preionization fractions  $x_e = 0.1-0.6$  between  $z = 15$  and 10, with large comoving rates of star formation,  $0.001-0.1 M_{\odot} \text{ Mpc}^{-3} \text{ yr}^{-1}$ , and baryon fractions,  $\omega_{\text{BH}} \approx 10^{-6}$  to  $10^{-5}$ , accreted onto black holes. Any significant contribution to  $\tau_e$  from X-ray preionization requires  $x_e \geq 0.1$ . Therefore, the lower value of  $\tau_e$  from *WMAP-5* reduces the allowed X-ray preionization and black hole accretion rates significantly compared to these models. Ricotti et al. (2005) find that the IGM at  $z > z_{\text{GP}}$  was highly ionized ( $x_e \gg 0.01$ ). In this limit, there were few X-ray secondary electrons, and most of the X-ray energy went into heating the ionized medium. By contrast, the *WMAP-5* optical depth suggests that the IGM was much less ionized at  $z > z_{\text{GP}}$ .

Relating the effects of X-ray ionization from early black holes to a  $\Delta\tau_e$  and a related X-ray production efficiency factor is less straightforward compared to the star formation case, for the following reasons. First, unlike ionization by UV photons, X-ray ionization is nonequilibrium in nature, and the timescales for X-ray photoionization at any epoch prior to  $z = 6$  typically exceed the Hubble time at those epochs (VGS01). Therefore, it is more difficult to establish a one-to-one correspondence between X-ray production at an epoch and the average efficiency of halos. In addition, X-ray ionization (whether from stars or black holes), at least initially when  $x_e < 0.1$ , will be dominated by secondary ionizations from X-ray-ionized helium electrons (VGS01) rather than from direct photoionization. This may constrain the physical conditions in the IGM (e.g., the level of He ionization) rather than those in the parent halo, when we attempt to translate a  $\Delta\tau_e$  into an X-ray ionization efficiency. Thus, it may be difficult to make precise inferences about the black hole density and accretion history from  $\tau_e$ .

We can define an X-ray ionization rate and efficiency parameter, analogous to the previous case for massive star formation. We define  $x_e(z) = \epsilon_X f_b(z)$ , with no clumping factor, where  $\epsilon_X = N_X f_{\text{BH}} f_{\text{esc}}$  and  $f_b(z)$  is the fraction of baryons in collapsed halos. Here  $f_{\text{BH}}$  is the average fraction of baryons in black holes (BHs) in halos at  $z \geq 7$  and  $N_X$  is the number of X-ray ionizations of the IGM produced by X-rays and secondary ionizations, per baryon accreted onto such black holes. As we now describe,  $f_{\text{BH}}$  may approach  $10^{-4}$ , and standard accretion estimates give  $N_X \approx 10^6$  photons baryon $^{-1}$ , so that  $\epsilon_X \approx 100$ .

Ricotti & Ostriker (2004) and Ricotti et al. (2005) define a parameter  $\omega_{\text{BH}} = 10^{-7}$  to  $10^{-6}$ , equal to the fraction of baryons

that go into *seed* black holes. Current observations (e.g., Häring & Rix 2004) suggest that the BH-to-bulge mass fraction in modern galaxies is  $M_{\text{BH}}/M_{\text{bulge}} \approx 1.4 \times 10^{-3}$ . Thus, if the bulge-to-halo mass ratio is 0.065,  $f_{\text{BH}} \approx 10^{-4}$ , after BHs have grown from the initial fraction through accretion, thereby producing X-ray ionization at high  $z$ . To estimate  $N_X$ , we assume Eddington-limited accretion at 10% efficiency and adopt a mean photon energy  $\sim 1$  keV:

$$N_X \approx \left[ \frac{(12)0.1m_p c^2}{(1.6 \times 10^{-9} \text{ erg})E_{\text{keV}}} \right] \approx (10^6 \text{ photons baryon}^{-1})E_{\text{keV}}^{-1}. \quad (8)$$

Here we assume that each X-ray photon produces  $\sim 12$  hydrogen ionizations, primarily through secondary ionizations from X-ray photoelectrons (Shull & van Steenberg 1985; VGS01). In the partially ionized IGM, the free electrons come from  $\text{H}^+$ ,  $\text{He}^+$ , and trace  $\text{He}^{+2}$ . We assume that the clumping factor ( $c_L$ ) and escape fraction ( $f_{\text{esc}}$ ) are roughly unity for X-rays, given their high penetrating power relative to UV photons. Figure 2 shows the allowed additional optical depth, analogous to the constraints of Figure 1, for X-ray efficiency in both  $\text{Ly}\alpha$ -cooled halos and minihalos. Evidently, X-rays from black holes located in high-redshift minihalos can produce  $\Delta\tau_e \approx 0.02$ , with a substantial ionizing efficiency,  $\epsilon_X \approx 100$ , that rivals that of Pop II star formation.

In summary, we have shown that the revised (*WMAP*-5) values of CMB optical depth,  $\tau_e = 0.084 \pm 0.016$ , lead to a more constrained picture of early reionization of the IGM. Approximately half of the observed  $\tau_e$  comes from a fully ionized IGM back to  $z_{\text{GP}} \approx 6-7$ . The additional  $\Delta\tau_e$  at  $z > z_{\text{GP}}$  probably arises from the first massive stars and from accretion onto early black holes. Some of the observed  $\tau_e$  may come from scattering from residual electrons left from recombination; inaccuracies in computing this ionization history add systematic uncertainty to

the CMB inferred signal. We have assumed extra scattering,  $\Delta\tau_e = 0.03 \pm 0.02$ , at  $z > z_{\text{GP}}$  and used this to constrain the efficiencies for production and escape of ionizing photons, either by ultraviolet photons from the first massive stars (Fig. 1) or by X-rays from accretion onto early black holes (Fig. 2).

In both cases, the picture is of a partially ionized IGM at redshifts  $z = 6-20$ . For X-ray preionization by early black holes, equation (6) can be used to provide an estimate of the effects of partial reionization. Between redshifts  $z_2 \approx 20$  and  $z_1 \approx 6$ , an IGM with ionized fraction  $x_{e,0} = 0.1$  (Ricotti et al. 2005) would produce  $(\Delta\tau_e) = (0.018)(x_{e,0}/0.1)$ , which is a significant contribution to the observed  $\tau_e = 0.084 \pm 0.016$ . Ricotti et al. (2005) suggested a large  $x_e \approx 0.1-0.6$  and pushed their black hole space densities and accretion rates to large values in order to reach the *WMAP*-1 estimates of  $\tau_e = 0.17$ . Because such large values of  $\tau_e$  are no longer required, the black hole densities and IGM ionization fractions are likely to be considerably less.

All these constraints depend heavily on uncertain parameterizations of the efficiency of star formation and ionizing photon production. The most sensitive of these parameters is  $\sigma_8$ , although the details of the clumping factor are comparably important. With more precise measurements of CMB optical depth from future missions, there is hope that more stringent constraints on high- $z$  star formation and black hole accretion will be possible. These data include additional years of *WMAP* observations, as well as the *Planck* mission.

We are grateful to David Spergel, Licia Verde, Rachel Bean, and Nick Gnedin for useful discussions regarding the interpretation of *WMAP* data and numerical simulations. We thank Douglas Scott and Wan Yan Wong for providing their calculations of recombination history. This research at the University of Colorado was supported by astrophysical theory grants from NASA (NNX07-AG77G) and NSF (AST 07-07474).

#### REFERENCES

- Alvarez, M., Shapiro, P. R., Ahn, K., & Iliev, I. 2006, *ApJ*, 644, L101  
 Becker, R., et al. 2001, *AJ*, 122, 2850  
 Begelman, M. C., Volonteri, M., & Rees, M. J. 2006, *MNRAS*, 370, 289  
 Benson, A. J., Sugiyama, N., Nusser, A., & Lacey, C. 2006, *MNRAS*, 369, 1055  
 Cen, R. 2003, *ApJ*, 591, L5  
 Cen, R., & Ostriker, J. P. 1999, *ApJ*, 519, L109  
 Chluba, J., & Sunyaev, R. A. 2008, *A&A*, 480, 629  
 Ciardi, B., Ferrara, A., & White, S. D. M. 2003, *MNRAS*, 344, L7  
 Dunkley, J., et al. 2008, *ApJS*, submitted (arXiv:0803.0586)  
 Fan, X., et al. 2002, *AJ*, 123, 1247  
 ———. 2006, *AJ*, 132, 117  
 Gnedin, N. Y. 2000, *ApJ*, 535, 530  
 ———. 2004, *ApJ*, 610, 9  
 Gnedin, N. Y., & Fan, X. 2006, *ApJ*, 648, 1  
 Gnedin, N. Y., & Ostriker, J. P. 1997, *ApJ*, 486, 581  
 Häring, N., & Rix, H.-W. 2004, *ApJ*, 604, L89  
 Haiman, Z., & Bryan, G. L. 2006, *ApJ*, 650, 7  
 Haiman, Z., & Holder, G. P. 2003, *ApJ*, 595, 1  
 Hallman, E. J., O'Shea, B. W., Burns, J. O., Norman, M. L., Harkness, R., & Wagner, R. 2007, *ApJ*, 671, 27  
 Hinshaw, G., et al. 2008, *ApJS*, submitted (arXiv:0803.0732)  
 Hu, E., & Cowie, L. L. 2006, *Nature*, 440, 1145  
 Hu, E., et al. 2002, *ApJ*, 568, L75  
 Hui, L., & Haiman, Z. 2003, *ApJ*, 596, 9  
 Kodaira, K., et al. 2003, *PASJ*, 55, L17  
 Kogut, A., et al. 2003, *ApJS*, 148, 161  
 Kohler, K., Gnedin, N. Y., & Hamilton, A. J. S. 2007, *ApJ*, 657, 15  
 Komatsu, E., et al. 2008, *ApJS*, submitted (arXiv:0803.0547)  
 Kriss, G. A., et al. 2001, *Science*, 293, 1112  
 Peimbert, M., Luridiana, V., & Peimbert, A. 2007, *ApJ*, 666, 636  
 Ricotti, M., Gnedin, N. Y., & Shull, J. M. 2002a, *ApJ*, 575, 33  
 ———. 2002b, *ApJ*, 575, 49  
 Ricotti, M., & Ostriker, J. P. 2004, *MNRAS*, 350, 539  
 Ricotti, M., Ostriker, J. P., & Gnedin, N. Y. 2005, *MNRAS*, 357, 207  
 Ricotti, M., & Shull, J. M. 2000, *ApJ*, 542, 548  
 Seager, S., Sasselov, D., & Scott, D. 2000, *ApJS*, 128, 407  
 Seljak, U., & Zaldarriaga, M. 1996, *ApJ*, 469, 437  
 Shull, J. M., Tumlinson, J., Giroux, M. L., Kriss, G. A., & Reimers, D. 2004, *ApJ*, 600, 570  
 Shull, J. M., & van Steenberg, M. E. 1985, *ApJ*, 298, 268  
 Sokasian, A., Abel, T., Hernquist, L., & Springel, V. 2003, *MNRAS*, 344, 607  
 Sokasian, A., Yoshida, N., Abel, T., Hernquist, L., & Springel, V. 2004, *MNRAS*, 350, 47  
 Spergel, D. N., et al. 2003, *ApJS*, 148, 175  
 ———. 2007, *ApJS*, 170, 377  
 Tegmark, M., & Silk, J. 1995, *ApJ*, 441, 458  
 Tumlinson, J. 2006, *ApJ*, 641, 1  
 Tumlinson, J., Venkatesan, A., & Shull, J. M. 2004, *ApJ*, 612, 602 (TVS04)  
 Umeda, H., & Nomoto, K. 2003, *Nature*, 422, 871  
 Venkatesan, A. 2006, *ApJ*, 641, L81  
 Venkatesan, A., Giroux, M. L., & Shull, J. M. 2001, *ApJ*, 563, 1 (VGS01)  
 Venkatesan, A., Tumlinson, J., & Shull, J. M. 2003, *ApJ*, 584, 621 (VTS03)  
 Wyithe, J. S. B., Bolton, J. S., & Haehnelt, M. G. 2008, *MNRAS*, 383, 691  
 Wyithe, J. S. B., & Loeb, A. 2003, *ApJ*, 586, 693  
 Zaldarriaga, M. 1997, *Phys. Rev. D*, 55, 1822  
 Zheng, W., et al. 2004, *ApJ*, 605, 631